Vol. 38 No. 3 Journal of the Communications Research Laboratory November 1991
Printed in Tokyo, Japan pp. 553 – 575

IV. EXPERIMENTAL RESULTS

IV. 5 A RADIO SOURCE CATALOG OBTAINED BY VLBI

By
Yukio TAKAHASHI

(Received on March 18, 1991)

ABSTRACT

The Kashima station in Japan has participated in many domestic and international Very Long Baseline Interferometry (VLBI) experiments such as Crustal Dynamics Project (CDP) experiments, Jet Propulsion Laboratory (JPL) experiments, Japan-Australia-Hawaii joint experiments. These experiments supplied data of extra-galactic sources such as the source positions, the correlated amplitude and the resolution of the structure, as described in this paper.

The celestial reference frame defined by the positions of extra-galactic sources is essentially immovable as compared with other celestial frames. This celestial frame is suitable for measuring, for example, the proper motion of other sources, earth rotation and movement of stations on the earth's surface. The positions of 46 sources are estimated with high precision (0.1 mill arcsec: mas) from 82 CDP experiments from 1984 to 1988. The reference point of the frame is the right ascension of the point-like source (0229 + 131). Changes in position of 3C273B, 3C345, 3C454.3, 4C39.25 and OJ287 are found. The source positions of 28 sources in the southern hemisphere are estimated with precision better than 10 mas in the Japan-Australia-Hawaii experiments.

The correlation amplitudes of sources are obtained on both long baselines greater than 1000 km and a 55 km short baseline in Japan. Three values are newly introduced as a catalog item to indicate the resolution of source structure, its time variation, and the change in flux density. Large variation in flux density is observed for all quasars.

Absolute correlation flux density is obtained for 20 sources on the 55 km short baseline. The correlated fluxes of 28 new sources in the southern hemisphere are also obtained on the long baseline.

1. Introduction

The Communications Research Laboratory (CRL) has conduced many geodetic VLBI experiments since 1984. The positions and movements (plate motion) of stations have been measured very precisely from these experimental data[1]. Precise positions of radio sources (quasars) have also been obtained. The quasars are located very far from our galaxy, beyond 10 billion parsec (pc), and their relative positions are thought to be essentially immovable. A reference frame based on these radio source positions is thus considered to be the most desirable of all coordinate systems. To construct a reference frame, a source position catalog has been prepared based on experiments held from 1984 to 1988 including the Kashima station. The difference in source positions due to different analysis

methods was examined and found to be very small.

Many catalogs of radio sources have been prepared using data observed by Very Long Array (VLA) and/or VLBI. Familiar catalogs are those compiled by Goddard Space Flight Center (GSFC), National Geodetic Survey (NGS) and JPL. The precision of the former two catalogs is better than 0.1 mas. However, differences between the catalogs can be as much as 0.5 mas even after correction of systematic frame rotation caused by different reference definitions. These catalogs include sources mainly in the northern hemisphere. On the other hand, the JPL catalog includes sources in the southern hemisphere in addition to those in the northern hemisphere, although the number of sources from $-20°$ to $-40°$ in declination is few. Its precision is about 1 mas less than that of GSFC and NGS catalogs.

The correlated flux catalog by Morabito[2] includes 416 sources obtained by VLBI and VLA measurements. However, precision of the positions in the catalog is low, 10 mas or worse. Thus, these are no catalog having correlated flux and resolution of structure in addition to position data. A combined catalog including all of this information would be very helpful for preparing VLBI observation schedules. In response to this need, we have begun work on such a combined catalog and report on new results for source positions and source flux in this paper.

2. Source Positions

2.1 Precise Source Catalog

The positions of 46 sources were estimated by using 82 VLBI experiments in which Kashima participated from 1984 to 1988. The CDP experiments were mainly analyzed. Figure 1 shows a typical observation network. The main stations were Kashima (Japan), Gilcreek (Alaska), Kauai (Hawaii) and

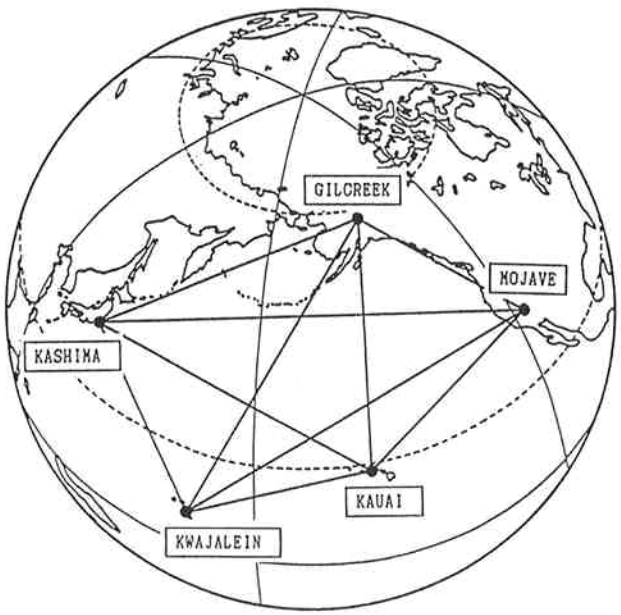

Fig. 1 CDP observation network around the Pacific.

Table 1 Source Positions obtained by Japan-USA joint VLBI experiments (1984–1988) (J2000.0 system)

Source name	Right ascention Adjusted value (HH	MM	SS)	Error	Declination Adjusted value (HH	MM	SS)	Error
0106+013	1	8	38.77107	0.000003	1	35	0.3181	0.00006
0208–512	2	10	46.20040	0.000213	–51	1	1.8900	0.00151
0212+735	2	17	30.81378	0.000009	73	49	32.6211	0.00004
0229+131	2	31	45.89409	–	13	22	54.7162	0.00005
0234+285	2	37	52.40574	0.000002	28	48	8.9895	0.00004
0300+470	3	3	35.24237	0.000009	47	16	16.2750	0,00009
3C84	3	19	48.16013	0.000019	41	30	42.1029	0.00027
0420–014	4	23	15.80069	0.000002	–1	20	33.0656	0.00006
0528+134	5	30	56.41676	0.000003	13	31	55.1486	0.00008
0537–441	5	38	50.36180	0.000189	–44	5	8.9411	0.00175
0552+398	5	55	30.80563	0.000002	39	48	49,.1632	0.00003
0727–115	7	30	19.11233	0.000008	–11	41	12.5997	0.00014
0823+033	8	25	50.33830	0.000019	3	9	24.5187	0.00071
OJ287	8	54	48.87488	0.000002	20	6	30.6395	0.00004
4C39.25	9	27	3.01380	0.000003	39	2	20.8503	0.00003
1034–293	10	37	16.07958	0.000057	–29	34	2.8115	0.00061
1144+402	11	46	58.29779	0.000004	39	58	34.3043	0.00006
1156+295	11	59	31.83379	0.000007	29	14	43.8263	0.00009
3C273B	12	29	6.69970	0.000002	2	3	8.5996	0.00005
1308+326	13	10	28.66376	0.000004	32	20	43.7834	0.00006
1334–127	13	37	39.78266	0.000009	–12	57	24.6915	0.00016
1354+195	13	57	4.43658	0.000008	19	19	7.3733	0.00012
OQ208	14	7	0.39431	0.000004	28	27	14.6911	0.00007
1418+546	14	19	46.59715	0.000014	54	23	14.7879	0.00014
1424–418	14	27	56.29732	0.000096	–42	6	19.4344	0.00063
1502+106	15	4	24.97977	0.000004	10	29	39.2011	0.00014
1548+056	15	50	35.26922	0.000003	5	27	10.4513	0.00006
1633+38	16	35	15.49288	0.000008	38	8	4.5023	0.00008
1637+574	16	38	13.45617	0.000007	57	20	23.9809	0.00007
3C345	16	42	58.80986	0.000002	39	48	36.9959	0.00003
NRAO530	17	33	2.70572	0.000010	–13	4	49.5438	0.00027
1739+522	17	40	36.97774	0.000024	52	11	43.4100	0.00021
1741--38	17	43	58.85613	0.000003	–3	50	4.6130	0.00009
1749+096	17	51	32.81856	0.000003	9	39	0.7314	0.00007
1803+784	18	0	45.68369	0.000005	78	28	4.0205	0.00002
1921–293	19	24	51.05597	0.000015	–29	14	30.1170	0.00030
1958–179	20	0	57.09034	0.000061	–17	48	57.6674	0.00086
3C418	20	38	37.03481	0.000024	51	19	12.6648	0.00021
2113+293	21	15	29.41347	0.000023	29	33	38.3690	0.00060
2121+053	21	23	44.51738	0.000004	5	35	22.0959	0.00008
2134+00	21	36	38.58631	0.000004	0	41	54.2159	0.00010
2145+067	21	48	5.45867	0.000003	6	57	38.6066	0.00005
VR42201	22	2	43.29145	0.000004	42	16	39.9816	0.00005
2216-038	22	18	52.03770	0.000003	–3	35	36.8764	0.00009
2234+282	22	36	22.47091	0.000009	28	28	57.4151	0.00015
3C454.3	22	53	57.74795	0.000002	16	8	53.5626	0.00004
2326–477	23	29	17.70475	0.000127	–47	30	19.1180	–

Mojave (California) around or on the Pacific ocean. Other stations were Hatcreek, Vandenberg (California), Kwajallein (Marshall islands), Haystack, Westford (East Coast), Richimond (Florida), Wettzell (Germany), Onsala (Sweden), Sheshan (China) and DSS45 (Australia).

The reference of our catalog was the right ascension of 0229+131 (2h31m45.89409s in J2000.0 system) taken from the GLOBAL solution of the GSFC group[3], whose reference was the right ascension of 3C273B (12h29m6.6997s in J2000.0 system), which we still used as a primary reference. The right ascension of 3C273B has long been the reference for the celestial frame since the position connected with the dynamical frame defined by earth orbit and rotation through measurements of lunar occultation. However, 3C273B has a very changeable structure famous for "super luminal expansion," which could affect source positions measured by VLBI. We thus felt that the reference should be a point-like source[4], and chose 0229+131 since its change in position by change in structure is considered to be very small or nonexistent.

The other parameters and source positions were estimated in our analysis. Station positions were measured from 1984 to 1988 and we found that their movements well fit the linear change due to plate motion. Therefore, station positions at the epoch (1984.1.1) and plate motions were estimated. In addition, the positions of DSS45 and Sheshan were estimated for each experiment since the data period was too short to estimate the plate motion. The earth rotation parameters (UTI, wobble), nutations, clock change and atmospheric delay were also estimated for every experiment (local estimation). Table 1 shows the 46 source positions estimated according to the procedure described above. The estimated error was very small, below 0.1 mas for all sources.

The obtained source positions were compared with the latest GSFC catalog[5]. The reference of this latter catalog was the mean of several source positions obtained by optical observations, which was different than the right ascension of 3C273B. Table 2 shows the difference between the two catalogs. We can see a large rotation of 5.2 mas around the Z axis arising from different reference.

Table 2 Difference between our catalog and the new GSFC catalog

Rotation of coordinate	
X axis	0.14 ± 0.08 mas
Y axis	-0.74 ± 0.08 mas
Z axis	5.22 ± 0.06 mas
R.M.S. of residuals	
Right ascension	0.38 mas
Declination	0.40 mas

Table 3 Difference in source positions by various analysis methods (r.m.s.)

	Right ascension	Declination
Elevation cut off >20 degrees	0.08 mas	0.24 mas
No estimation of plate motion	0.01 mas	0.05 mas
No estimation of ERP	0.59 mas	0.92 mas
Estimation of every experiments for some source positions	0.08 mas	0.24 mas

There was also a small rotation of –0.7 mas around the Y axis in spite of estimating the nutations for each experiment. The difference in relative source positions between the two catalogs was 0.4 mas for both right ascension and declination after removing coordinate rotation. This value was very small, but it was four times larger than the estimated precision. The accuracy of the obtained source positions should be 0.2~0.5 mas.

Source positions were estimated by several different methods to examine the dependence of position on estimation method. These methods were: (1) elevation cut-off test, that is, observations made above 20° in elevation were used for estimation; (2) plate motions were not estimated but station positions were estimated for each experiment (local estimation of station positions); (3) earth rotation parameters (ERP) were not estimated; and (4) the positions of sources whose structures are suspected to be resolved, such as 3C273B, 3C345, 3C454.3, OJ287, 4C39.25, were estimated for each experiment (source structure). The source positions obtained by these methods are compared in Table 3. The difference were at most 0.3 mas except for case (3). We could thus conclude that different estimation methods did not seriously affect the relative source positions.

2.2 Changes in Source Position

Changes in position of some sources which have a resolved structure were investigated. Figures 2 and 3 show changes in right ascension and declination for 3C273B and 3C345. Table 4 summarizes

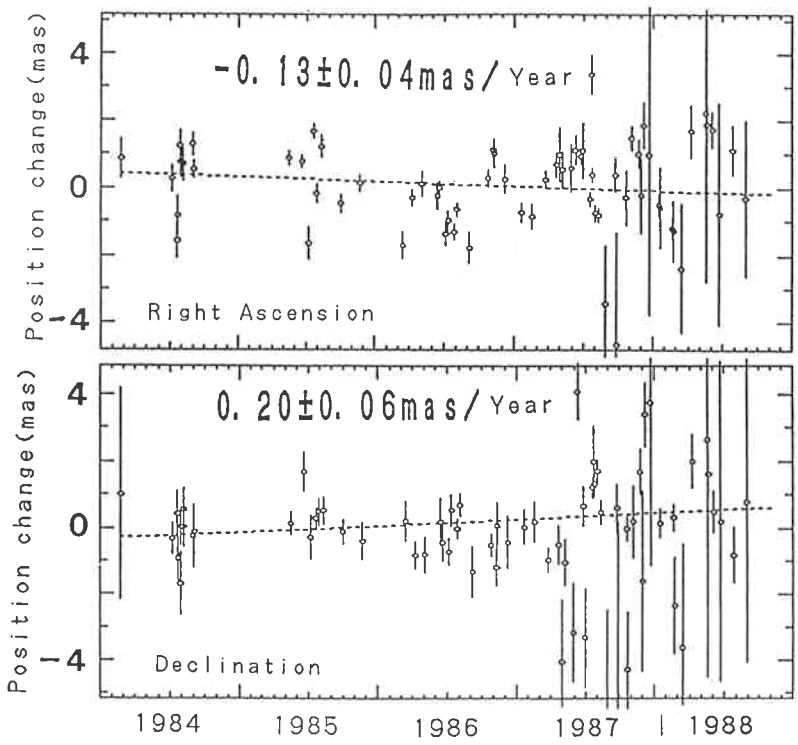

Fig. 2 Position change of 3C273B (unit: mas). (upper figure: right ascension, lower figure: declination)

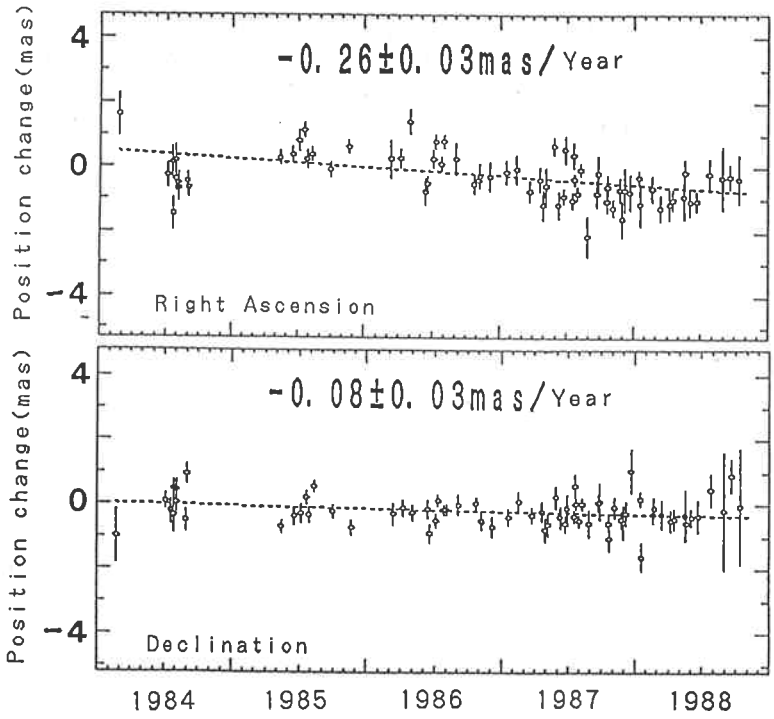

Fig. 3 Position change of 3C345 (unit: mas). (upper figure: right ascension, lower figure: declination)

Table 4 Changes in source positions

Source Name	Right ascension (mas/year)	Declination (mas/year)
3C273B	−0.13 ± 0.04	0.20 ± 0.06
3C454.3	−0.19 ± 0.02	−0.03 ± 0.03
3C345	−0.26 ± 0.03	−0.08 ± 0.03
OJ287	0.00 ± 0.03	0.02 ± 0.04
4C39.25	−0.05 ± 0.04	−0.15 ± 0.03

the rate of change in position for 3C273B, 3C345, 3C454.3, OJ287 and 4C39.25. Since these rates are several times larger than one sigma, changes in some source positions are considered to exist in spite of the very small rates of changes (0.1~0.2 mas/year). One interpretation is change in structure. If the core of a source is fixed and other parts of the source extend far from the core like jet phenomena, the source size becomes large and the mean source position changes. Another interpretation is direct movement of the relative source position as in superluminal expansion[6]. However, quasars are

extremely far from earth and this interpretation may be difficult to support. Continuous monitoring of such structures is both necessary and interesting.

2.3 Source Positions in the Southern Hemisphere

In the CDP experiments, the number of sources observed in the southern hemisphere was few. Special experiments were therefore conducted with the Hawaii, Kashima, and Australia stations to measure the position of sources mainly in the southern hemisphere, especially in the declination range from –20° to –40°. We called the experiments "SOUTH." The experiments were conducted on 15th and 16th December 1988, 23th April 1989 and 8th June 1989. The station positions and clock and atmospheric delays were estimated for each experiment. The positions of the new 28 sources (see Table 5) were measured from these experiments. Their precision was about 2 mas in right ascension

Table 5 Positions of the sources in the southern hemisphere obtained by SOUTH experiments (J2000.0 system)

Source name	Right ascention			Error	Declination			Error
0118–272	1h	20m	31.66332s	1.7	–27°	1'	24.6495"	0.7
0135–247	1h	37m	38.34617s	2.6	–24°	30'	53.8830"	1.1
0150–334	1h	53m	10.12168s	1.7	–33°	10'	25.8587"	0.7
0202–172	2h	4m	57.67428s	2.0	–17°	1'	19.8420"	1.3
0220–349	2h	22m	56.40140s	2.8	–34°	41'	28.7298"	1.5
0426–380	4h	28m	40.42436s	1.9	–37°	56'	19.5835"	1.2
0528–250	5h	30m	7.96270s	1.7	–25°	3'	29.8975"	0.6
0537–441	5h	38m	50.36149s	7.1	–44°	5'	8.9403"	3.1
0629–418	6h	31m	11.99824s	8.0	–41°	54'	26.9555"	3.1
0637–337	6h	39m	20.90454s	3.2	–33°	46'	0.1131"	0.6
0646–306	6h	48m	14.09650s	2.2	–30°	44'	19.6658"	1.1
0818–128	8h	20m	57.44757s	1.1	–12°	58'	59.1693"	0.4
0826–373	8h	28m	4.78036s	1.5	–37°	31'	6.2802"	0.7
0920–397	9h	22m	46.41852s	2.9	–39°	59'	35.0753"	2.0
1048–313	10h	51m	4.77780s	2.5	–31°	38'	14.3147"	1.4
1101–325	11h	3m	31.50480s	–	–32°	51'	16.7190"	2.1
1104–445	11h	7m	8.69396s	5.9	–44°	49'	7.6221"	3.0
1143–245	11h	46m	8.10381s	2.8	–24°	47'	32.9034"	1.3
1206–399	12h	9m	35.26923s	–	–40°	16'	13.0830"	1.0
1255–316	12h	57m	59.06103s	2.1	–31°	55'	16.8555"	1.2
1451–375	14h	54m	27.40994s	2.0	–37°	47'	33.1375"	1.0
1451–400	14h	54m	32.91301s	3.7	–40°	12'	32.5160"	1.9
2000–330	20h	3m	24.11659s	2.6	–32°	51'	45.1275"	1.3
2037–253	20h	40m	8.77311s	3.5	–25°	7'	46.6623"	1.8
2106–413	21h	9m	33.18968s	6.5	–41°	10'	20.6076"	2.3
2149–306	21h	51m	55.52409s	2.3	–30°	27'	53.6943"	1.2
2312–319	23h	14m	48.50140s	–	–31°	38'	39.5264"	0.6
2329–384	23h	31m	59.47597s	3.9	–38°	11'	47.6439"	1.7

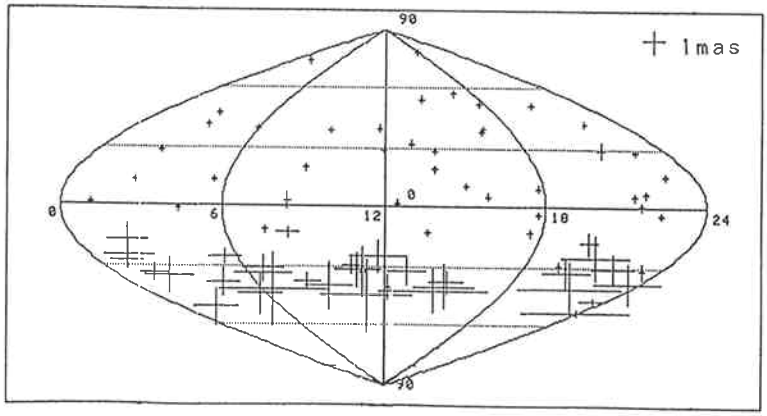

Fig. 4 Distribution of the sources in our catalog and position error (size of + is position error).

and 1 mas in declination. The worse precision in right ascension was due to the baseline configurations, i.e., the long north-south and short east-west baseline components.

Figure 4 shows the derived source positions with the error bars of one sigma. As shown, the sources in our catalog are distributed uniformly in the celestial sphere north of –50° declination.

3. Correlated Amplitudes and Source Structure

The expected values of correlation amplitudes are employed to evaluate the duration of observation when a schedule is made up. In addition to correlated amplitudes, source structure information is also important to select sources adequate for geodetic VLBI. A source catalog including the above information can thus be very useful when scheduling observations. Correlation amplitudes and resolution of source structure depend on the sensitivity of each antenna and *UV* (where *U* is the projection of the baseline in the right ascension direction and *V* is the projection of the baseline in the declination direction). *UV* changes by the length and direction of the baseline and by observation time. Correlated amplitudes and resolution of source structure also depend on the baseline and observation time. Up to now, the changes in structure and flux density have not been made clear quantitatively. New values for the resolution and time variation of the correlated flux are introduced here.

To obtain general purpose values, five standard baselines are selected. One baseline is a long baseline to obtain high resolution data, because the *UV* value is larger as the baseline is longer. Data on an east-west baseline is more suitable to study source structure than that on a north-south baseline. This is because the fringe visibility (the resolution factor of the source structure) does not change significantly over a day on the north-south baseline, and the change in UV on an east-west baseline is greater than that on a north-south baseline. A north-south baseline, however, is necessary to obtain data for large V. On the earth, a mutually visible sky narrows with an increase in baseline, so that a middle length (about 5000 km) baseline is adequate for studying source structure. Hence, we define an east-west baseline about 8000 km in length as the first standard baseline (hereafter referred to as B1). The next two standard baselines are 5000 km baselines in length in east-west (B2) and north-south

(B3) directions. The forth standard baseline is taken to be a 2000 km east-west baseline (B4). The fifth baseline is a 100 km short baseline (B5) to obtain data under low resolution interferometer conditions, which is considered here to be similar to total flux density. In our experimental results, B1 is the Kashima-Mojave east-west 8100 km baseline; B2 is the Kashima-Kauai east-west 5700 km baseline; B3 is the Kauai-Gilcreek north-south 4700 km baseline; B4 is the Kashima-Shanghai east-west 1900 km baseline; and B5 is the Kashima-Tsukuba 50 km short baseline. In addition to these, the Kashima-Gilcreek 5700 km baseline is also used in our results.

The correlated amplitude $\rho(\%)$ is given by

$$\rho = L\frac{\pi}{8k} D_1 \cdot D_2 \sqrt{\frac{\eta_1 \cdot \eta_2}{T_1 \cdot T_2}}\, r \cdot S, \qquad \ldots\ldots\ldots\ldots\ldots\ldots\ldots\ldots\ldots\ldots\ldots\ldots (1)$$

where D (m) is antenna diameter, T (K) is system temperature, η is antenna efficiency, r is the resolution factor of source structure, L is the coherence factor, k is Boltzmann's constant and S (Jy) is flux density of the source. The suffixes 1 and 2 denote reference and remote interferometer antenna, respectively. In the case of only system temperature noise, $L = 1$. However, there is coherence loss caused by frequency instability, scintillation of propagation and correlation processing. The resolution factor of the source structure, its time variance, the change in correlated flux and the ratio of correlated flux against that of the reference source are obtained from the correlated amplitudes at X band (8 GHz) on each baseline. The elevation dependency of the system temperature is not corrected here and it does not seriously affect current results, although its effect will be discussed later.

3.1 Resolution of Source Structure

Some sources, such as 3C273B and 3C345, are resolved at X band on a long baseline (>2000 km). The effect of source structure on correlated amplitude is evaluated here numerically.

The resolution of source structure is a function of both U and V. Data obtained for various UV combinations in a 24-hour experiment can provide information about the source structure. For example, the standard deviation of correlated amplitude indicates the resolution for each source. The correlated amplitude is dependent upon the system temperature, the coherence loss and the resolution factor, as indicated by Eq. (1). The change in correlated amplitude is related to the mean of these parameters, that is, the standard deviation of correlated amplitudes increases as this mean increases. The correlated standard deviation is normalized by the mean of the correlated amplitudes to study the resolution factor of the source structure. This normalized value A is the percentage of structure effect on the correlated amplitude, and is given by

$$A = \frac{(\text{Standard deviation of correlated amplitudes})}{(\text{Mean of the correlated amplitudes})}$$

$$= \frac{\sqrt{\sum_{j=1}^{N} \left(\rho_j(i) - \overline{\rho}(i)\right)^2 / N}}{\overline{\rho}_{(i)}}, \qquad \ldots\ldots\ldots\ldots\ldots\ldots\ldots\ldots\ldots\ldots\ldots\ldots (2)$$

where $\rho_j(i)$ is the correlated amplitude (j: observation number for the source, i: experiment number),

$\overline{\rho}(i)$ is the mean of them in each experiment ($\overline{\rho}(i) = \sum_{j=1}^{N} \rho_j(i)/N$), and N is the number of observations for the source in a particular experiment. A is calculated on each baseline for each experiment. Table 6 shows the mean value of A for sources providing large amounts of data in our analysis. The efficiency, source flux and the constant value appear in both denominator and numerator of Eq. (2), and are thus canceled out. The coherence loss by atmospheric scintillation and the system temperature depend on elevation and weather conditions. The elevation dependency of system temperature is not corrected, but the change is less than 10% at X band, in general. The coherence loss by atmospheric scintillation is 8% at X-band for an integration time of 400 sec and the atmospheric scintillation of 1.0×10^{-13} as a standard value. In fact, the mean value of A for several sources is less than 10%. This means that the effects of coherence loss and system temperature on the correlated amplitudes is considered to be less than 10%. Therefore A can be approximated as

$$A = \frac{\sqrt{\sum_{j=1}^{N} \left(r_j(i) - \overline{r}(i)\right)^2 / N}}{\overline{r}(i)} \qquad \cdots\cdots\cdots\cdots\cdots\cdots\cdots\cdots\cdots\cdots\cdots\cdots\cdots\cdots\cdots\cdots (3)$$

where $\overline{r}(i)$ is the mean of the resolution factor in each experiment ($\overline{r}(i) = \sum_{j=1}^{N} r_j(i)/N$, where $r_j(i)$ is the resolution factor of all observation). (A) means the percent resolution of the source structure on each baseline. When it is beyond 10%, the structure is resolved.

Assuming that the source structure is single gauss distribution, the typical size (s) of the source can be calculated by the dependency of the correlated amplitudes on ($U^2 + V^2$) so as to fit the following

Table 6 Effect of the resolved structure on correlated flux (1984–1988) (%)

Source name	KAS–GIL	KAS–KAU	GIL–KAU	KAS–MOJ	KAS–TSU
0106 + 013	16.9	15.7	23.1	10.2	5.8
0212 + 735	21.6	18.2	14.3	27.9	–
0229 + 131	7.1	5.7	7.0	8.6	5.0
0234 + 285	13.6	13.2	8.5	15.9	5.9
0420 – 014	8.6	7.1	7.6	7.7	6.5
0528 + 134	11.0	7.7	9.6	18.1	–
0552 + 398	13.9	14.7	12.0	11.9	10.4
OJ287	13.5	10.6	13.4	9.0	10.4
4C39.25	30.8	29.8	33.5	18.2	12.7
3C273B	29.4	29.9	46.8	24.2	9.9
OQ208	15.9	19.0	29.3	20.9	4.6
1548 + 056	7.8	8.0	14.5	9.5	2.3
3C345	49.5	42.0	27.0	32.9	13.2
1741 – 038	7.4	5.8	7.7	8.5	–
1749 + 096	7.1	8.6	6.8	4.6	–
1803 + 784	12.8	12.7	16.8	15.6	8.4
2134 + 004	10.6	–	–	11.4	9.8
2145 + 067	9.9	7.5	10.8	8.5	7.9
3C454.3	21.1	23.6	19.4	15.6	9.5

equation (4):

$$In(\rho) = \alpha - \beta\left(U^2 + V^2\right)$$
$$\beta = (\pi \cdot s)^2 / \ln 2. \qquad \ldots\ldots\ldots\ldots\ldots\ldots\ldots\ldots\ldots\ldots\ldots\ldots\ldots\ldots\ldots\ldots (4)$$

The size is a physical value and the correlated amplitude is estimated for any *UV*. However, this assumption cannot be made for all sources, and the change in correlated amplitudes needs *UV* and some calculation. (*A*) is used in our results to estimate the correlation amplitudes. In the future, the size of the source will also be included in our catalog.

The means of *A* are within 10% for all sources on the short baseline (Kashima-Tsukuba 55 km baseline), and it is considered that the structures of all sources except for 3C84 are not resolved on this baseline. On baseline longer than 5000 km, the mean value of *A* exceeds 10%, as in the case of 3C345, 3C273B and 4C39.25, whose mean values are greater than 30%. This indicates that the sources are highly resolved. Although the Kashima-Mojave baseline is long, the standard deviation is smaller than other baselines for some sources since mutual visibility is limited. Long baselines greater than 8000 km are not suitable to study source structures. The means of *A* for 0106 + 013, 0212 + 735, 0234 + 285, 3C273B, OQ208 and 3C345 are different between Kashima-Kauai (east-west) baseline and Gilcreek-Kauai (north-south) baseline. If the structure is a symmetric single gauss distribution or point-like source, correlated amplitudes on east-west baselines are the same as those on north-south baselines. Therefore, the difference indicates the structure of the sources are asymmetric or complex. On the other hand, the mean values of 0229 + 131, 0420 – 014, 1548 + 056, 1741 – 038, 1749 + 096 and 2145 + 067 are within 10% on all baselines. These sources are considered to be point-like sources, and are hence suitable for the reference sources of geodetic VLBI experiments.

3.2 Time Variation of the Source Structure

The time variation of the source structure is investigated here. The *UV* coverage on each baseline is almost the same for all experiments. If there is no change in the structure, the variation of resolution factors is the same for all experiments. Since *A* is approximated as a function only of the resolution factor as expressed by Eq. (3), *A* is almost constant for all experiments and the standard deviation of *A* is small.

In general, quasars will have a resolved structure consisting of a core and some subcomponents (for example jets), or they will appear to have a gauss distribution whose size is greater than the resolution. (*A*) structure change (except for an unusual drastic change) means a change in subcomponents and a change in intensity ratio between the core and subcomponents. The size of the core is almost the same. If there is a long-term change in structure, the standard deviation of resolution factors in each experiment, which is the numerator of Eq. (3), changes. On the other hand, the mean of the resolution factors, which is the denominator of Eq. (3), hardly changes since the contributions of the subcomponents on the resolution factors are canceled out in a experiment and the mean value is mainly contributed to by the core. The standard deviation of *A* indicates the long-term change in structure (Table 7).

The standard deviations are small for the unresolved sources mentioned in section 3.1 (0229 + 131, 0420 – 014, 1548 + 056, 1741 – 038, 1749 + 096, 2145 + 067). Although some sources, such as 0212 + 735, 0234 + 285, 0552 + 398, OJ287, OQ208 and 1803 + 784, are resolved, their standard

Table 7 Effect of the time variation of the structure (1984–1988) (%)

Source name	KAS–GIL	KAS–KAU	GIL–KAU	KAS–MOJ	KAS–TSU
0106 + 013	11.6	8.7	15.2	8.3	0.6
0212 + 735	7.7	5.4	5.7	10.2	–
0229 + 131	5.8	2.8	3.1	7.7	3.7
0234 + 285	7.4	5.5	4.3	8.3	1.2
0420 – 014	4.8	6.2	6.2	7.9	4.5
0528 + 134	11.6	4.2	8.5	14.2	–
0552 + 398	6.9	4.7	3.9	7.2	5.5
OJ287	6.5	6.9	7.6	7.1	2.4
4C39.25	21.4	12.8	14.3	8.9	6.9
3C273B	21.9	16.5	10.7	15.4	3.8
OQ208	7.8	4.3	3.5	6.1	3.1
1548 + 056	4.7	3.8	7.9	9.3	3.2
3C345	19.5	17.0	8.0	9.7	8.1
1741 – 038	4.1	3.1	4.9	8.9	–
1749 + 096	6.4	6.7	3.1	2.5	–
1803 + 784	5.9	4.0	3.3	6.4	2.6
2134 + 004	5.9	–	–	3.1	2.7
2145 + 067	4.7	5.2	5.0	6.2	3.1
3C454.3	17.0	13.2	12.2	9.7	3.8

deviations are small, within 10%. Therefore, the structures are considered to be stable. On the other hand, both the mean values and the standard deviations of A are large for 0106 + 013, 0528 + 134, 4C39.25, 3C273B, 3C345 and 3C454.3. These sources are resolved and have a changeable structure. As information on structure change is useful for the study of quasars, these sources should be observed frequently. It is possible that changes in structure affects not only the positions of sources but also the geodetic VLBI results. Sources must thus be point-like sources and have no long-term change in structure for geodetic VLBI.

3.3 Change in Correlated Flux

The change in flux density S is not only necessary for estimating correlated amplitudes when preparing observation schedules, but is also important for research of source characteristics. The following value B is calculated for 19 sources to obtain the change in correlated flux (Table 8).

$$B = \frac{\left(\begin{array}{l}\text{Standard deviation of the mean values}\\ \text{of correlated amplitudes for each experiment}\end{array}\right)}{\left(\begin{array}{l}\text{Mean value of the mean values}\\ \text{of correlated amplitudes for each experiment}\end{array}\right)}$$

$$= \frac{\sqrt{\sum_{i=1}^{n}\left(\bar{\rho}(i)-\bar{\rho}\right)^2 / n}}{\bar{\rho}}, \qquad (5)$$

where $\overline{\rho}(i)$ is the mean of correlated amplitudes for each experiment ($\overline{\rho}(i) = \sum_{j=1}^{N} \rho_j(i)/N$, where $\rho_j(i)$ is the correlated amplitude, j is observation number for the source, N is the number of observations for the source in a particular experiment), i is experiment number, and n is the number of experiments. $\overline{\rho}$ is the mean of $\overline{\rho}(i)$ ($\overline{\rho} = \sum_{i=1}^{n} \overline{\rho}(i)/n$).

The constant value of correlated amplitude in Eq. (1) appears in both a denominator and numerator and is thus canceled out. The mean of correlated amplitudes for each experiment depends on the mean value of coherence loss and system temperature for each experiment. Although these mean values change mainly due to weather conditions, the change in the mean correlated amplitude caused by the effects is considered to be less than 10% since the coherence loss by atmospheric scintillation itself is less than 10% at X-band and since the mean of system temperature also changes less than 10% in general. Therefore B can be described only by the resolution factor r and the flux density S as follows:

$$B = \frac{\sqrt{\sum_{i=1}^{n} \left(\overline{r}(i)S(i) - \overline{r \cdot S}\right)^2 / n}}{\overline{r \cdot S}}, \qquad \ldots\ldots\ldots\ldots\ldots\ldots\ldots\ldots\ldots\ldots\ldots\ldots (6)$$

where S(i) is the flux density and $\overline{r}(i)$ is the mean of the resolution factor for each experiment. The term $\overline{r \cdot S}$ is the mean of the correlated flux density ($\overline{r \cdot S} = \sum_{i=1}^{n} \overline{r}(i)S(i)/n$).

The mean of resolution factors hardly changes, if the *UV* coverage is wide, as described in Subsection 3.2. Therefore, B can be expressed in only the flux density S as

$$B = \frac{\sqrt{\sum_{i=1}^{n} \left(S(i) - \overline{S}\right)^2 / n}}{\overline{S}}, \qquad \ldots\ldots\ldots\ldots\ldots\ldots\ldots\ldots\ldots\ldots\ldots\ldots (7)$$

where $\overline{S}$ is the mean of the flux density for all experiments ($\overline{S} = \sum_{i=1}^{N} S(i)/n$). The value in Table 8 is considered to be the variation in flux density.

The value B exceeds 30% for most sources on baselines longer than 5000 km (KAS-KAU, KAU-GIL, KAS-GIL, KAS-MOJ). This fact strongly suggests that the flux density of a region within 2–3 mas, which is the resolution of a 5000 km baseline, is changeable. The value B for a particular source is almost the same for all baselines.

We have investigated the change in the correlated amplitude on three baselines between Kashima, Kauai and Gilcreek to examine the change in the flux density S in detail. The changes in the correlated amplitudes are the same for each of these baselines for a particular source, each of which exhibit different behavior, except for 3C273B and 3C345. If the change in correlated flux is caused by a change in the antenna system performance or by the source structure, the behavior should be different for every baseline. Therefore, the changes common to these three baselines must be caused by the change in flux density of the source.

The changes in correlated amplitude of five sources, 0106 + 013, 0552 + 398, OJ287, 4C39.25, 1803 + 784 and 3C454.3, are large and common to the three baselines. Figures 5 to 10 show the change

Table 8 Change in the correlated flux (1984–1988) (%)

Source name	KAS–GIL	KAS–KAU	GIL–KAU	KAS–MOJ	KAS–TSU
0106 + 013	26.3	33.7	24.8	27.5	16.5
0212 + 735	9.3	6.4	10.2	20.3	–
0229 + 131	23.8	25.2	17.3	25.1	10.6
0234 + 285	50.2	49.8	61.3	44.8	17.1
0420 – 014	24.7	18.0	13.0	32.2	13.1
0528 + 134	31.3	24.7	18.1	49.9	–
0552 + 398	18.8	19.9	27.1	23.0	21.1
OJ287	29.3	33.2	19.0	30.5	13.9
4C39.25	41.3	34.6	37.0	22.9	19.0
3C273B	41.4	34.9	18.3	40.9	28.6
OQ208	9.8	6.7	12.1	15.8	3.3
1548 + 056	18.4	14.9	36.4	11.0	10.0
3C345	28.7	23.2	17.8	26.6	30.5
1741 – 038	12.9	4.4	14.2	13.5	–
1749 + 096	21.9	19.9	22.7	41.6	–
1803 + 784	20.7	20.8	28.4	21.2	13.5
2134 + 004	32.0	–	–	22.7	12.6
2145 + 067	19.3	19.7	27.6	17.6	3.3
3C454.3	41.7	32.3	22.8	47.7	30.7

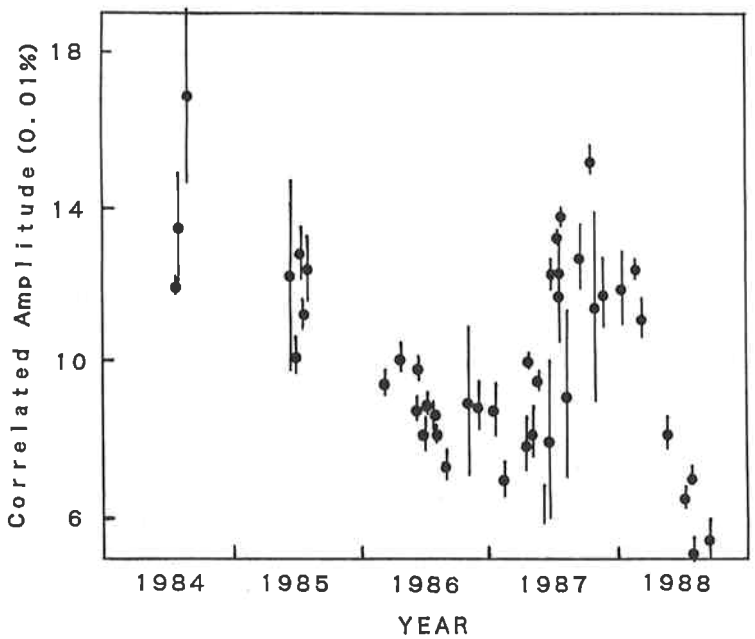

Fig. 5 Change of correlated amplitudes (flux) for 0106 + 013 on Kashima-Gilcreek (unit: 0.01%).

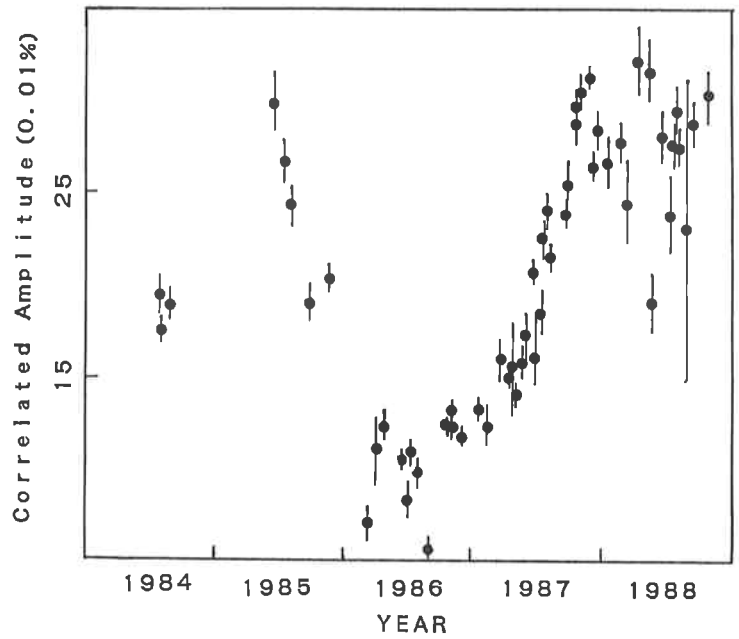

Fig. 6 Change of correlated amplitudes (flux) for 1803 + 784 on Kashima-Gilcreek (unit: 0.01%).

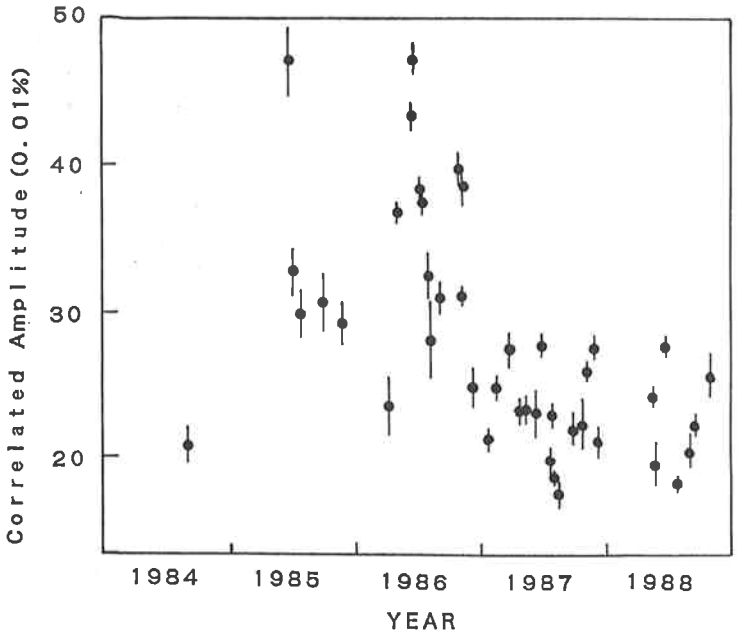

Fig. 7 Change of correlated amplitudes (flux) for OJ287 on Kashima-Gilcreek (unit: 0.01%).